Hindawi
International Journal of Photoenergy
Volume 2020, Article ID 8813688, 15 pages
https://doi.org/10.1155/2020/8813688

Research Article

Rectangular Glass Optical Fiber for Transmitting Sunlight in a Hybrid Concentrator Photovoltaic and Daylighting System

Afshin Aslian,[1] **Kok-Keong Chong**,[2] **Seyed Hassan Tavassoli**,[3] **Chin-Joo Tan**,[1] **and Omid Badkoobe Hazave**[3]

[1]*Department of Mechanical Engineering, Faculty of Engineering, University of Malaya, Malaysia*
[2]*Department of Electrical and Electronic Engineering, Lee Kong Chian Faculty of Engineering and Science, Universiti Tunku Abdul Rahman, Bandar Sungai Long, 43000 Kajang, Selangor, Malaysia*
[3]*Department of Condensed Matter, Faculty of Laser and Plasma Research, Shahid Beheshti University, Iran*

Correspondence should be addressed to Chin-Joo Tan; tancj@um.edu.my

Received 6 June 2020; Revised 1 October 2020; Accepted 29 October 2020; Published 26 November 2020

Academic Editor: K. R. Justin Thomas

In this paper, we propose to use glass optical fibers with a rectangular cross-section for the application in a concentrator photovoltaic and daylighting system (CPVD) due to the unique characteristics of rectangular fibers with the capability to provide a uniform rectangular beam shape and a top-hat profile at the output. A mathematical model of rectangular optical fibers has been formulated in this study for different incident angles, and the results are compared with those of round optical fibers. Furthermore, the performance of the bundle of RGOFs is compared with that of the bundle of round optical fibers via simulation by using the ray-tracing method. The mathematical modelling and numerical simulation have demonstrated that the RGOF has advantages in terms of the improvement in relative transmission and reduction in energy leakage for the transmission through the optical fiber. The simulation result also shows that a higher flux of sunlight can be transmitted via the bundle of RGOFs as compared to the bundle of round optical fibers due to the higher coupling efficiency. The experiment results on the relative transmission in different incident angles for both round optical fibers and RGOFs have validated both the simulation and the mathematical modelling. The beam profile of our fabricated RGOF has also been measured via our laboratory facility. The flexibility test on the fabricated RGOF has been carried out to bend at a radius of 150 mm and twist at 90° at a fiber length of 2.2 m.

1. Introduction

The initial idea of the optical fiber used for transmitting sunlight can be dated back to forty years ago [1]. Recently, significant advances in the technology of optical fibers have extended the application to transmit the sunlight with a wide band of electromagnetic waves. The application of transmitting sunlight by a round optical fiber and the bundle of round optical fibers have been studied [2–6]. The optical fibers can transmit sunlight with reasonable low loss for a distance fewer than 10 meters, but the optical loss in the optical fibers becomes noticeable at longer distances [7]. Considering the said limitation, there are still many applications especially transmitting daylight via fiber optics for residential and commercial buildings, which are still regarded as a promising method [7–9].

In transmitting sunlight through a dish and a round optical fiber, many components such as mirror accuracy and tracker precision, as well as the material, diameter, length, and type of optical fibers, can affect the efficiency of the whole system [10]. The material of the core and cladding of the optical fiber are the major factors to determine the acceptance angle of the optical fiber [11]. A parabolic dish with a high precision sun tracker can provide a solar concentration ratio of more than 8000 [12]. For transmitting the high flux of concentrated sunlight, a larger core diameter is usually

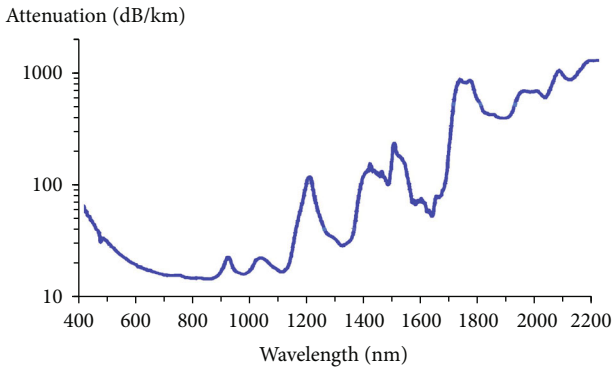

Figure 1: Attenuation of a typical square core optical fiber.

preferable. The one-millimeter core diameter of fused silica with a low refractive index of hard polymer resin as cladding can transmit a reasonable flux of sunlight with lower loss than that of polymer optical fibers [13, 14].

Transmitting sunlight with a wide spectrum of wavelengths via optical fibers encounters more challenges as compared to the application of optical fibers in telecommunications. The large core diameter of the optical fiber transmits light in multimode. The optical loss of the multimode fiber is higher in comparison to that of single-mode fibers made of the same material and transmitting the same wavelength of light [15]. Attenuation of power transmission in optical fibers with fused silica as the core and a hard polymer as the cladding is independent of the shape of the optical fiber [16]. Dugas et al. found that the leakage of power in sunlight transmission via a round optical fiber was attributed to optical loss due to too many reflections between the core and the clad with angles near the numerical aperture of the optical fiber [17]. To minimize the light leakage, the incident angle of sunlight relative to the numerical aperture of the optical fiber should be significantly less than the acceptance angle of the optical fiber. Feuermann et al. studied the dependence of light leakage within the nominal numerical aperture of the solar fiber optic on several parameters including incidence angle, optical properties of the core and cladding, and fiber length [13].

Moreover, the optical loss can occur when coupling the sunlight to a bundle of optical fibers. The method of bundling optical fibers will determine the amount of coupling loss. If a bundle of round optical fibers is fabricated by fusing all the optical fibers, the loss is lesser than that of the bundle of optical fibers being joined by epoxy adhesive. In the fusing process, the gaps among the optical fibers are diminished by forming one whole solid block, which has improved the coupling efficiency of light to the bundle of optical fibers [18]. However, the method of fusing optical fibers is much more expensive than by simply joining with epoxy adhesive.

A multijunction solar cell with a square dimension can convert sunlight into electricity in a concentrate photovoltaic (CPV) system. The dimensions of the multijunction cells that are available in the market are 3 mm × 3 mm, 5 mm × 5 mm, and 10 mm × 10 mm. Nevertheless, the matching between the concentrated light profile and the geometry of solar cells is essential to optimize the performance of the CPV system

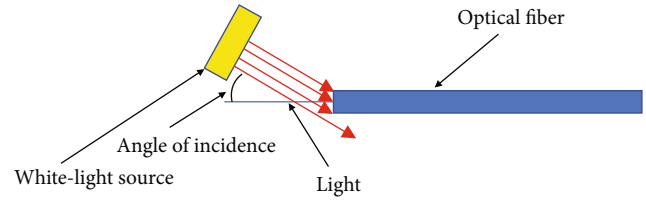

Figure 2: Setup of the tests for both round and flat fibers with the use of a rotating source.

[19]. Many works have been carried to study the design of solar concentrators for mapping the focused sunlight with the square shape of multijunction solar cells. Baig et al. and Yu et al. studied the compound parabolic concentrator (CPC) as a nonimaging concentrator to harness solar energy and mapping sunlight to square solar cells [20, 21]. A compound truncated pyramid and cone may be used for concentrating and coupling sunlight with the optical fiber. A bundle of optical fibers can be used as a coupler of concentrated sunlight to the multijunction solar cells in the CPVD system [12]. The optical fiber must be made of glass to tolerate the high temperature of concentrated light. A bundle of RGOFs with a square shape can map well the focused sunlight onto square solar cells.

Rectangular fibers were first studied for transmitting X-rays and light-wave circuit. Marcatili studied the rectangular waveguide for integrated optics in 1969 [22]. In the meantime, a square core optical fiber was developed for matching with the laser diode output beam. Cherny et al. (1979) studied waveguide characterization of a rectangular core and round clad for the cases of multi-mode and single-mode waves including the effect of single and double clads on dispersion of a pulse [23]. Blomster and Blomqvist studied square fiber for high-power laser applications in 2007 [24]. Konishi et al. developed a rectangular core optical fiber for a high-power laser in 2010 [25]. Ambran et al. demonstrated a physical micromachining technique to fabricate a flat fiber substrate for a light circuit [26]. The width of the flat fiber was 1612 μm, and the thickness of the core was about 10 μm.

Rectangular core fibers in the market have round clads. The core is made of fused silica for its broadband UV to NIR transmittance while the clad may be made of glass or a low refractive polymer. Figure 1 shows the attenuation of a square core in the market at different wavelengths. The core of the fiber is fused silica, and the clad is a hard polymer. These rectangular fibers are developed for applications in transmitting laser. The published data same as the published data of round optical fibers are extracted from propagating a beam of laser with a specific bandgap. Figure 1 reveals that attenuation is as low as 20 dB/km at 600 nm while the loss of fiber is more than the mentioned loss in transmitting sunlight.

In this paper, we would like to introduce RGOF that is specially designed for a CPVD system to transmit sunlight through the optical fiber. The core of RGOF can be fabricated by drawing a fused silica preform at the temperature of 2250°C. The preform must have a rectangular cross-section before drawing. The clad is a polymer with refractive index of 1.37 that is coated on the fused silica core. The length of

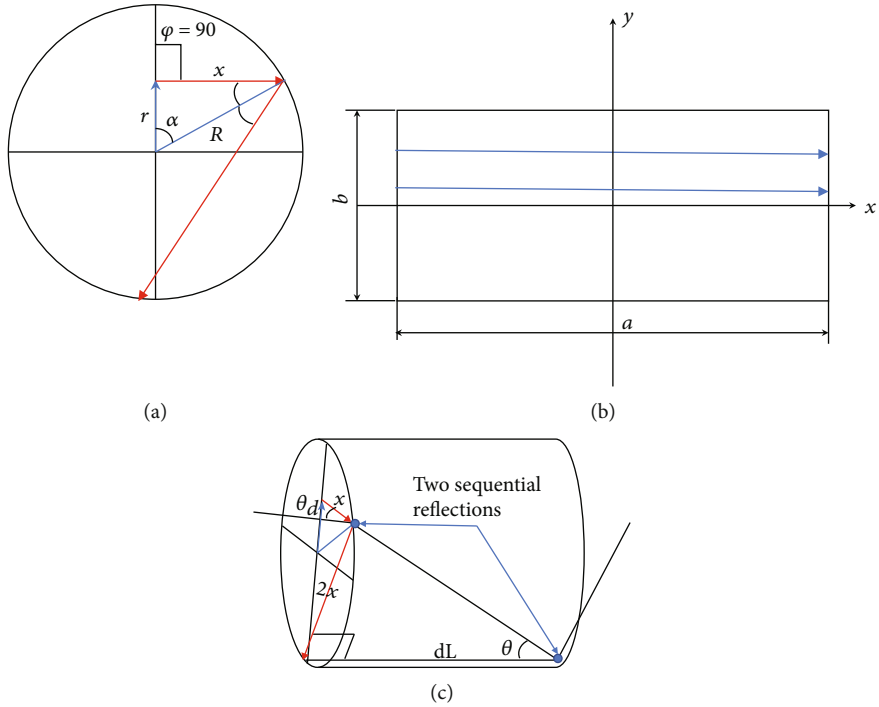

Figure 3: Incident angle of the ray trajectory direction relative to the plane normal to the (a) cross-sectional view of the round optical fiber, (b) cross-sectional view of the rectangular fiber, and (c) trajectory direction relative to the plane of the round optical fiber between two sequential reflections.

the rectangular core is between 5 mm and 10 mm with the width ranging from 0.2 mm to 0.5 mm. The thickness of the clad is about 0.1 mm.

The CPVD system has two functions including generating electricity and daylighting. The bundles of RGOF transmit sunlight from the focal point of the solar concentrator to the multijunction cells and the remote target. Furthermore, RGOF can also be used in other applications, i.e. sensors and delivery of a high-power laser beam.

A comprehensive manner composed of three major aspects embracing mathematical modelling, numerical simulation, and experimental verification is used for investigating the mechanism of leakage in transmitting sunlight in the RGOF. Based on previous studies, relative transmission of round optical fibers and RGOF in transmitting sunlight and the loss due to gaps between the fibers in a bundle are also studied. In Section 2, the mathematical model of the relative transmission is presented to compare between the round optical fiber and RGOF for different angles of incidence. In Section 3, the performance of RGOF is simulated by using the ray-tracing method. In Section 4, the effect of gaps is simulated for a bundle of RGOFs and the result is compared with that of a bundle of round optical fibers. In Section 5, the relative transmission, beam profile, and bending of the RGOF are investigated via experiments.

In this work, transmitting sunlight through an optical fiber with a rectangular glass core and a rectangular polymer clad has been investigated. Other researches on rectangular glass core fibers were only focused on the characterizations of the rectangular fiber for transmitting a high-power laser and pulse dispersion that involves a narrow band of wavelengths in the application of optical communication. For the originality of our study, the relative transmission of sunlight with a wide spectrum of wavelengths in the rectangular optical fiber is studied in a comprehensive manner in three major aspects embracing mathematical modelling, numerical simulation, and experimental verification.

2. Analytical Approach on Leakage of the Optical Fiber during Transmission of Sunlight

The efficiency of an optical fiber under the propagation of a full spectrum is different from the efficiency of the optical fiber under a collimated laser beam with a narrow bandgap. Manufacturers of optical fibers only provide information about the attenuation of light power at specific wavelengths but not the efficiency of transmitting a broad spectrum of light. The optical loss of an optical fiber with a specific attenuation varies with the length of the fiber. The light is coupled with the fiber with an incident angle of 0°. We may consider a source of light beam larger than the diameter of the optical fiber. If the angle of propagation increases up to the acceptance angle, the loss is changed with the cosine of incident angle. The loss of the fiber under the propagation of a wide spectrum for a specific incident angle is less than the expected loss. Feuermann measured the leakage of optical fibers under the propagation of a wide spectrum with different angles of propagation and different ratios of the length of the fiber to the diameter of the core.

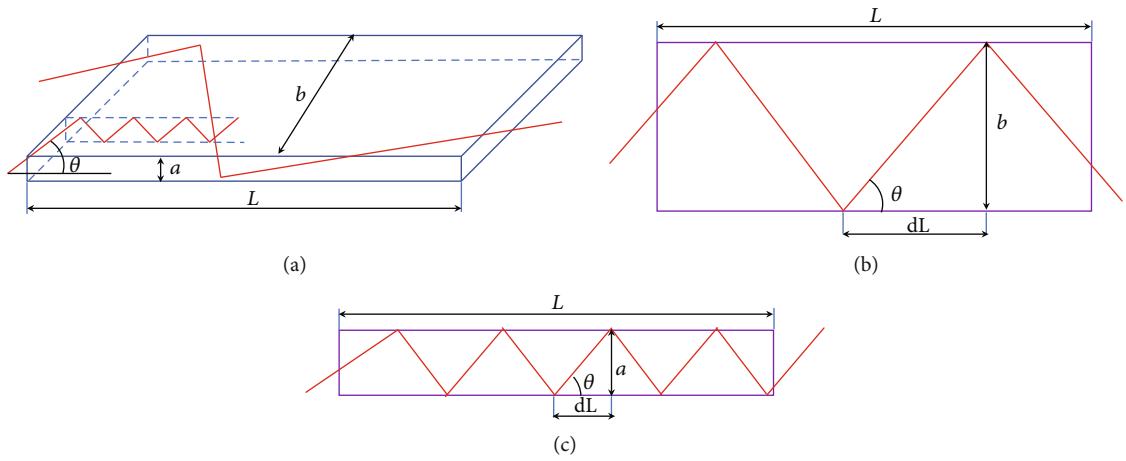

Figure 4: (a) Incident angle of the ray trajectory directions relative to the plane parallel to the axis of the rectangular fiber; (b) ray trajectory for the top view of the rectangular optical fiber; (c) ray trajectory for the side view of the rectangular optical fiber.

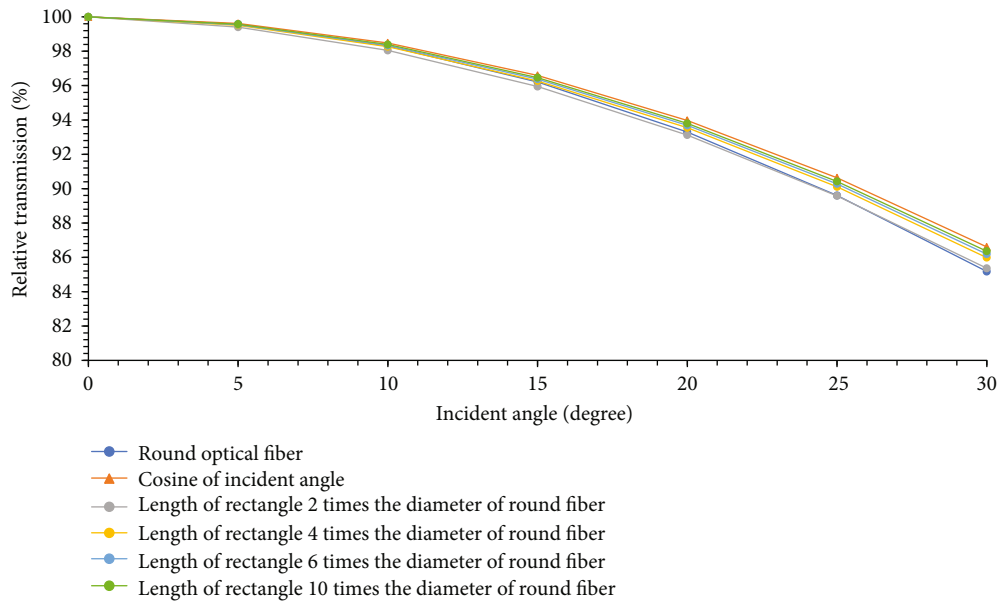

Figure 5: A comparison between the round fiber and rectangular fibers: $R_{av} = 0.9999$ and length = 100 mm.

For a fiber with a specific numerical aperture and specific angle of propagation, the ratio of the length of fiber to the diameter of the core directly affects the amount of leakage.

The mechanism of leakage in transmitting sunlight by optical fibers was studied, and it was found that the reflection of light between the core and the clad is not perfect and that the number of reflections of light determines the amount of leakage in the optical fiber. Concentrating sunlight leads to an increase in the incident angle between the rays of sunlight and the aperture of optical fibers. The number of reflections increases in such a condition, and the effect of the very small loss due to reflection is noticeable. The number of reflections increases with addition of the angle of incidence and the ratio of the length to the diameter of the fiber.

Although ray-tracing is a popular method, a mathematical analysis of loss is useful for understanding the behavior of fibers in various conditions and for assessing the accuracy of numerical methods. For the mathematical analysis of loss due to the number of reflections between the core and the clad, the optical fibers have been modelled to be exposed to the collimated light of a tilted source, which is likely to happen for the bundle of fibers used as the receiver of a CPVD system. Figure 2 shows the setup of a collimated light with an angle of incidence relative to the axis of the optical fiber. The average number of reflections for all rays is a variation that affects the relative transmission and determines the loss of the fiber due to the angle of incidence.

Figure 3(a) shows that the azimuth angle of the rays is 90° and the rays skew along the length of the fiber. Figure 3(b) shows the rays in the rectangular fiber. The rays in the round optical fiber skew around the axis of the fiber, but the rays move in a zigzag form in the rectangular fiber. Figure 3(c) shows the relation between $2x$, dL, θ, and θ_d in a round optical fiber.

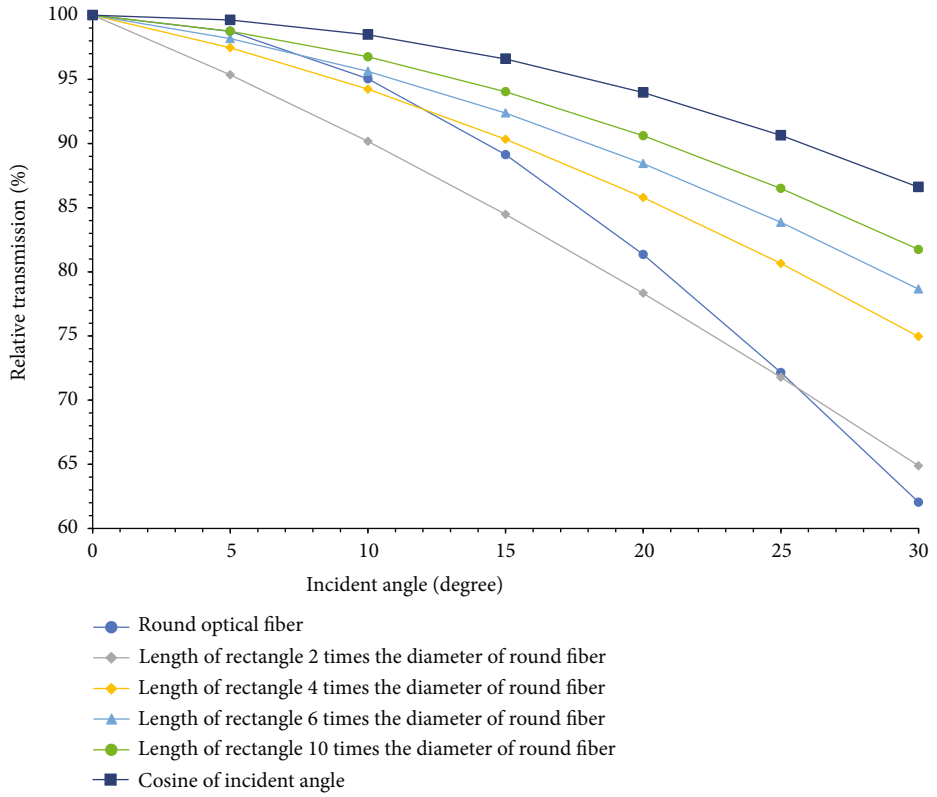

Figure 6: A comparison between round fiber and rectangular fiber: $R_{av} = 0.9999$ and the length = 10000 mm.

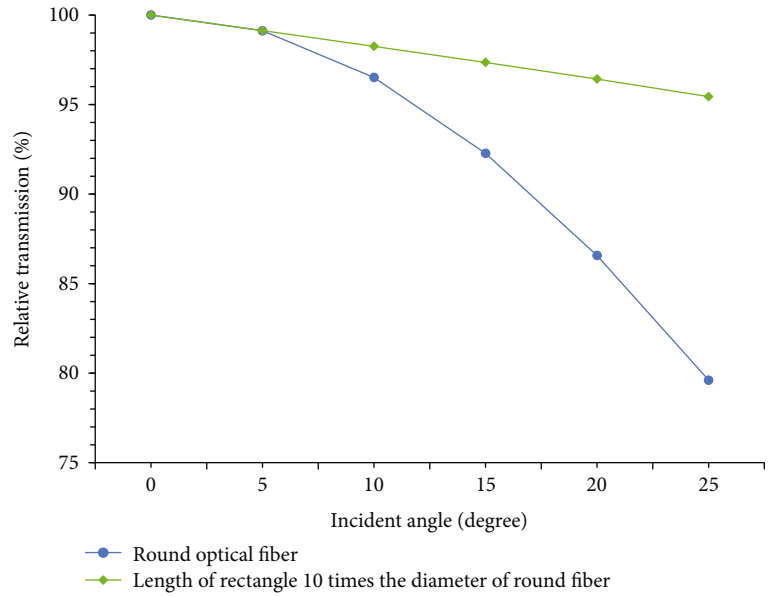

Figure 7: Comparison between round fiber and rectangular fiber: $R_{av} = 0.9999$, the length = 10000 mm, and diameter of the light = 1 mm.

Referring to Figures 2 and 3(a) for the case of the round optical fiber, we have

$$\sin \alpha = \frac{x}{R}, \qquad \tan \theta = \frac{2x}{dL}. \tag{1}$$

2x is the distance between two sequential reflections in the plane normal to the round optical fiber's axis. R is the radius of the optical fiber, and dL is the distance between two sequential reflections in the plane including a line parallel to the axis of the optical fiber and $2x$. θ is the angle between dL and the trajectory onto the plane through the dL including to 2x.

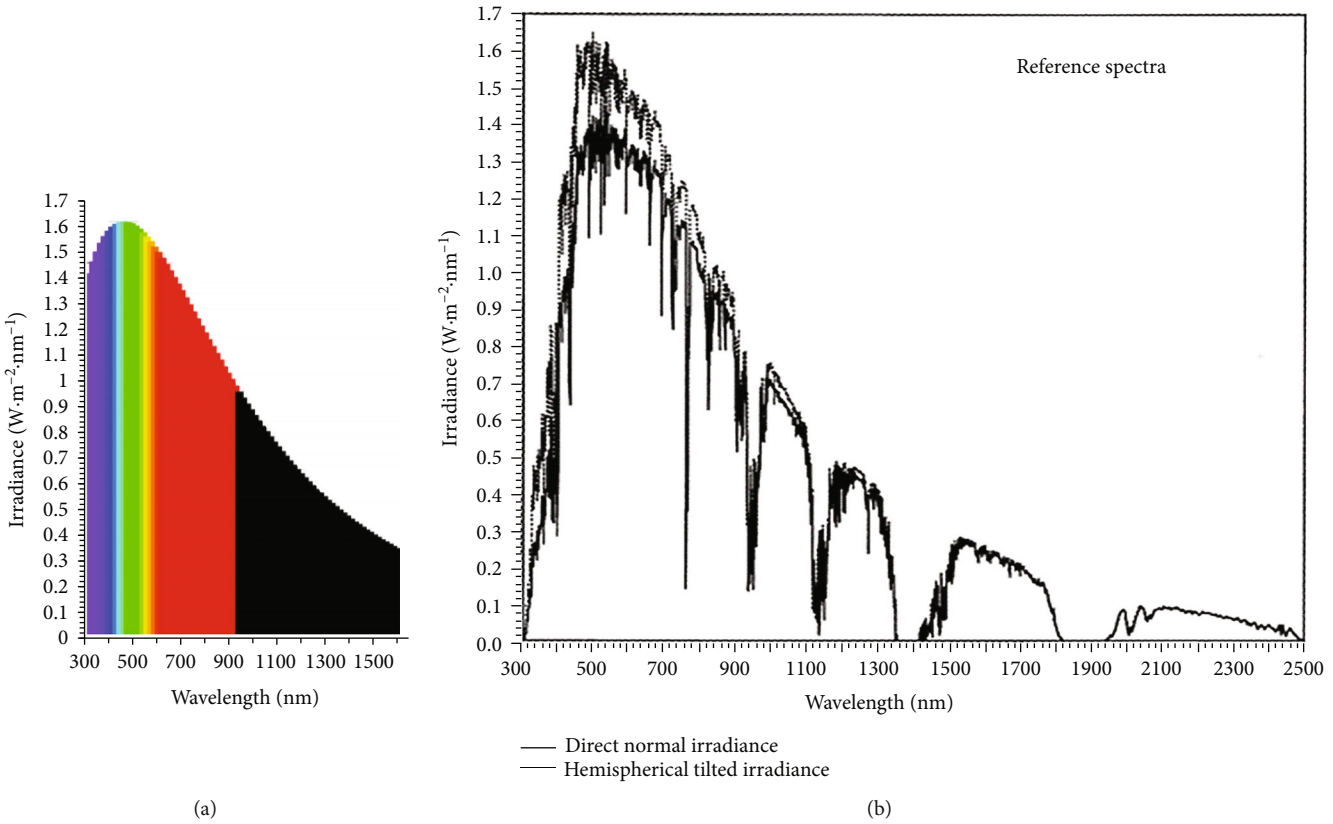

Figure 8: (a) The source file for the spectral irradiance of black body radiation at the temperature of 5780 K; (b) the direct normal irradiance of the standard AM 1.5 solar spectrum.

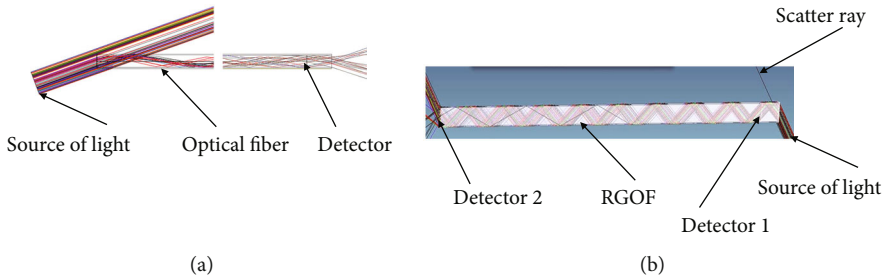

Figure 9: (a) Schematic diagram to show ray-tracing inside round optical fiber; (b) schematic diagram to show ray-tracing inside RGOF.

$$N_i = \frac{L \tan\theta}{d \sin\alpha}, \tag{2}$$

where N_i is the number of reflections for a ray in the length of the fiber, L is the length of the optical fiber, and d is the diameter of the fiber. The total number of reflections of all rays is

$$N_t = \int_0^{N_{\max}} N_i = \frac{L}{d}\int_0^{\theta_d}\int_{\alpha_{\min}}^{\pi/2}\int_0^{R}\int_0^{2\pi} \frac{\tan\theta}{\sin\alpha} d_\theta d_\alpha r d_r d_\omega, \tag{3}$$

where r and ω represent the polar coordinates of the interface of the fiber

$$N_t = \frac{L \times \pi d}{4} \ln|\cos\theta_d| \times \ln\left|\tan\frac{\alpha_{\min}}{2}\right|. \tag{4}$$

Considering the uniform distribution of rays on the surface of the interface of the fiber, we have

$$N_{\text{av}} = \frac{L}{d} \ln|\cos\theta_d| \times \ln\left|\tan\frac{\alpha_{\min}}{2}\right|, \tag{5}$$

where N_{av} is the average number of reflections for all rays. The angle of $\alpha_{\min}$ corresponds to the rays with the highest reflection and the lowest acceptable energy. We may consider that rays with a lower angle than $\alpha_{\min}$ are ignored. If the diameter of the propagated light is larger than the diameter of the optical fiber, then the power of incident light is

Table 1: Input data of simulation for both round optical fiber and RGOF.

	Round optical fiber	RGOF
Numerical aperture	0.39	0.39
Area of core	0.785 mm^2	5.0 mm^2
Source file	Blackbody radiation at 5780 K with 81 wavelengths ranging from 400 nm to 1600 nm	
Range of angle of incidence	0° to 25°	0° to 25°
Dimension of core	Diameter = 1 mm	0.5 mm × 10.0 mm
Dimension of clad	Diameter = 1.1 mm	0.6 mm × 10.1 mm
Material of core	Fused silica	Fused silica

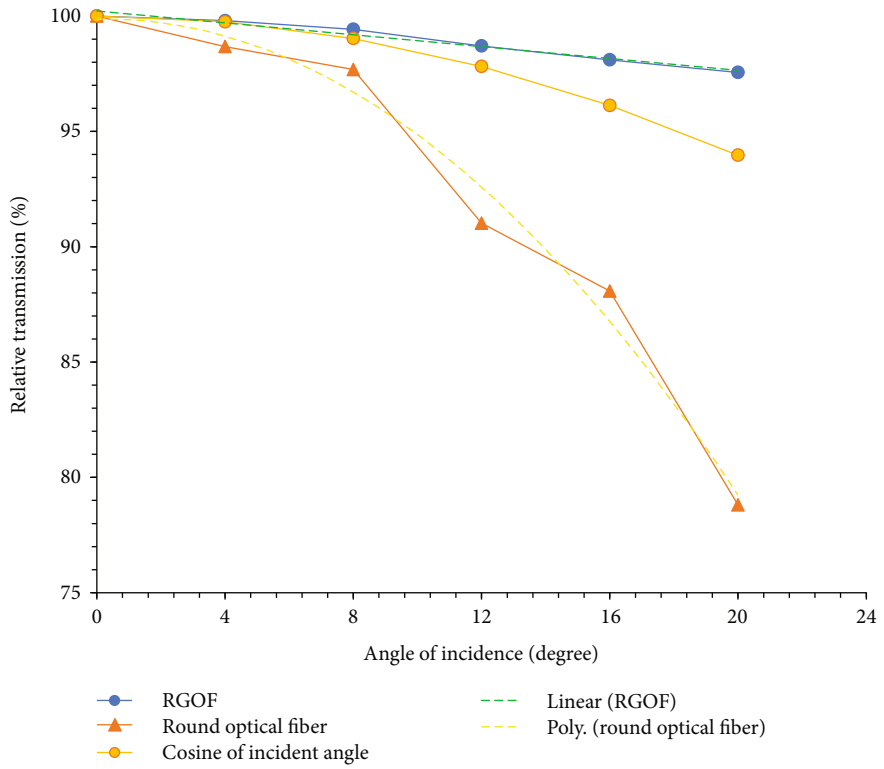

Figure 10: Simulation result of RGOF and round optical fiber with 1000 mm length.

proportional to the cosine of the incident angle. We have

$$\frac{\tau}{\tau_0} = \cos\theta_d R_{\text{av}}{}^{N_{\text{av}}}, \tag{6}$$

where R_{av} is the arithmetic average of reflectivity and θ_d is the angle of incidence relative to the axis of the optical fiber (see Figure 3). τ_0 is the transmission of the optical fiber at the angle of zero degree.

In the flat fiber, we do not have skew rays. The direction of the rectangular fiber to the propagated light determines the transmission of light in the zigzag direction. Figure 4(a) shows the effect of the zigzag direction on the number of reflections. Figure 4(b) shows the relation between the length of rectangle b, dL, and θ in a rectangular optical fiber. Figure 4(c) shows the relation between the width of rectangle a, dL, and θ in a rectangular optical fiber. Considering the independent reflections in both sides of the rectangular fiber, zigzag movement of the rays, and constant angle of reflection in each trajectory, we analyze the rectangular fiber in two dimensions of the rectangle. The average number of reflections on each side should be calculated separately; we have

$$\begin{aligned} \tan\theta &= \frac{b}{\text{dL}}, \\ N_i &= \frac{L\tan\theta}{a}, \end{aligned} \tag{7}$$

where a and b are the length and the width of the rectangular fiber, respectively.

$$N_t = \frac{L}{a}\tan\theta \int_0^a \int_0^b d_x d_y, \tag{8}$$

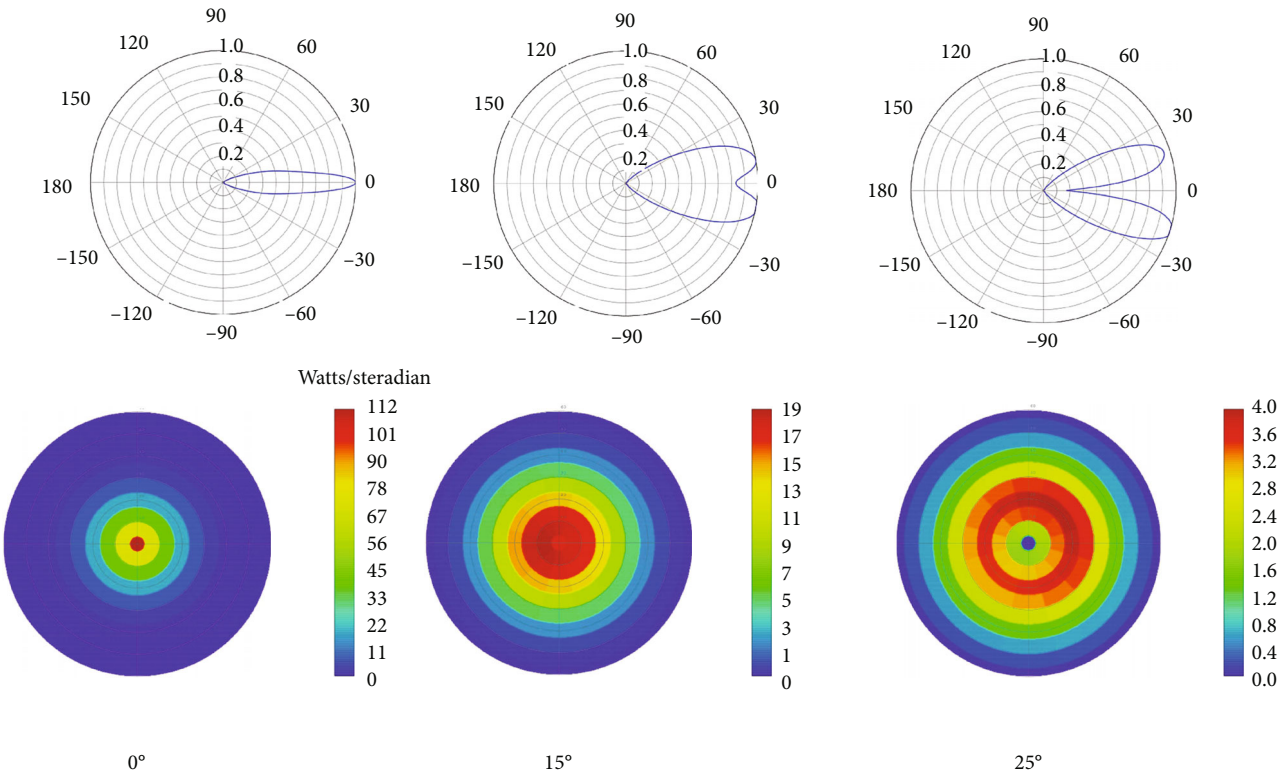

Figure 11: The radial intensity of the round optical fiber with different angles of the source.

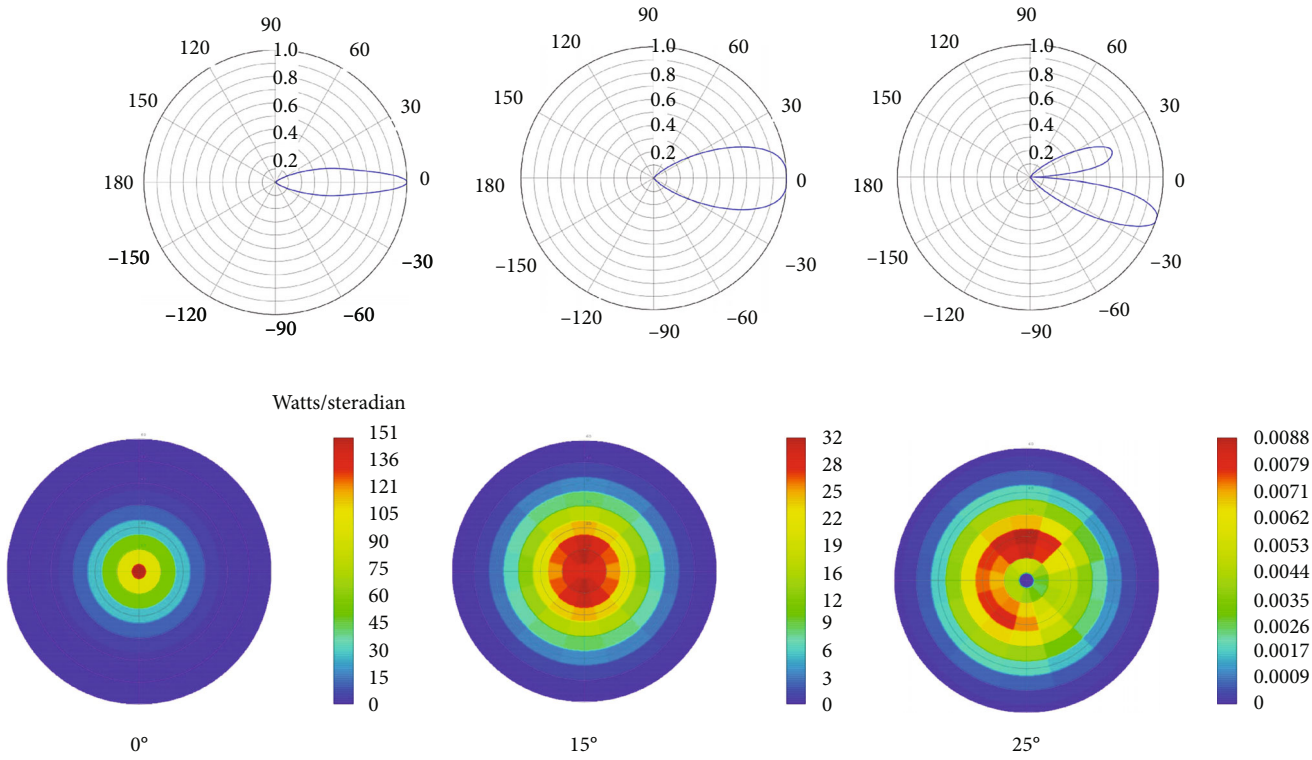

Figure 12: The radial intensity of RGOF with different angles of the source.

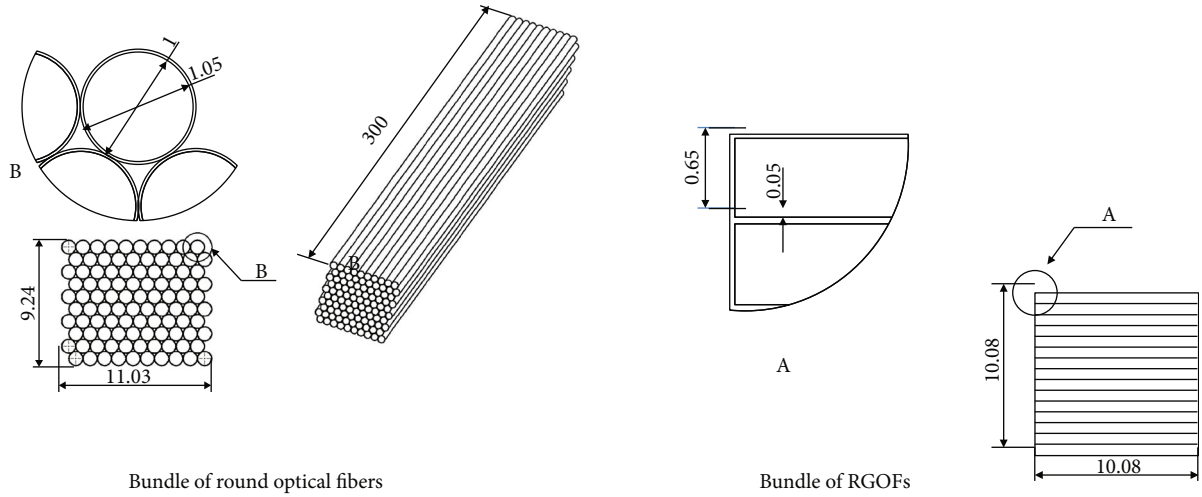

Figure 13: Dimensions of a bundle of RGOF fibers and a bundle of round optical fibers.

where dx and dy represent the Cartesian coordinate of the interface of the rectangular fiber

$$N_{\text{av}} = \frac{L \tan \theta}{a}. \tag{9}$$

For another side, we have

$$N_t = La \tan \theta,$$
$$N_{\text{av}} = \frac{L \tan \theta}{b}. \tag{10}$$

If the diameter of the propagated light is larger than the width of the rectangle in the fiber, then the power of incident light is proportional to the cosine of the incident angle. For one side, the relative transmission is

$$\frac{\tau}{\tau_0} = \cos \theta_d R_{\text{av}}^{(L/a) \tan \theta_d}. \tag{11}$$

For another side, the relative transmission is

$$\frac{\tau}{\tau_0} = \cos \theta_d R_{\text{av}}^{(L/b) \tan \theta_d}. \tag{12}$$

The direction of the rectangular fiber to the propagated light determines the zigzag transmission of light direction. Figure 4 shows that the direction of zigzag affects the number of reflections.

The designed RGOF is a glass optical fiber with a rectangular shape of the core and polymer clad; the ratio of the length to width of the rectangular fiber is more than 5 where the width must have a limit to prevent breakage during bending. As an example, the fabricated RGOF has a width or thickness of 0.4 mm and the minimum bending radius of 150 mm. If the diameter of the propagated light is large enough to cover the aperture of the optical fibers and the length of the fiber is to be short, the cosine of the incident angle plays an important role. Figure 5 shows the loss of a 100 mm length of a round fiber and a rectangular fiber where the light covers the aperture of the fibers. The diameter of the light is large enough and the cosine of angle of incidence should be considered. The ratio of the length of the rectangle to the diameter of the round fiber affects the relative transmission of the rectangular fiber. The effect of loss due to the number of reflections between the core and the clad is very low and the trends of optical fibers are near to each other and near to the cosine of the incident angle.

Figure 6 shows the relative transmission of fibers with a length of 10,000 mm, and light covers the surface of the fibers. The rectangular fiber with the length of the rectangle 10 times the diameter of the round fiber has a lower loss due to the number of reflections between the core and the clad and shows higher relative transmission than other fibers. The zigzag movement is in the longer trajectory (Figure 4).

If the diameter of the light is to be equal to the diameter of the round fiber, a rectangular fiber with the length of the rectangle 10 times the diameter of the round fiber shows higher relative transmission as compared to the round fiber. Figure 7 shows the relative transmission of a round and a rectangular fiber. The diameter of the round fiber is one millimeter, and the length of the rectangle of the rectangular fiber is 10 mm. the length of both fibers is 10,000 mm, and the diameter of the light is smaller than the diameter of the round fiber. The difference between the relative transmission of two fibers increases when the source is more tilted relative to the axis of the fiber.

3. Simulation of RGOF and Round Optical Fiber

The ray-tracing method has been applied to simulate the responses of the flat fiber (RGOF) and the conventional round fiber to a tilted source of light. For both cases of the flat and round fibers that consist of a fused silica core and a low refractive index resin clad, the parameters including the flux, relative transmission, and optical loss of the light have been investigated for different incident angles relative to the axis of the fiber, i.e., from 0° to 30°.

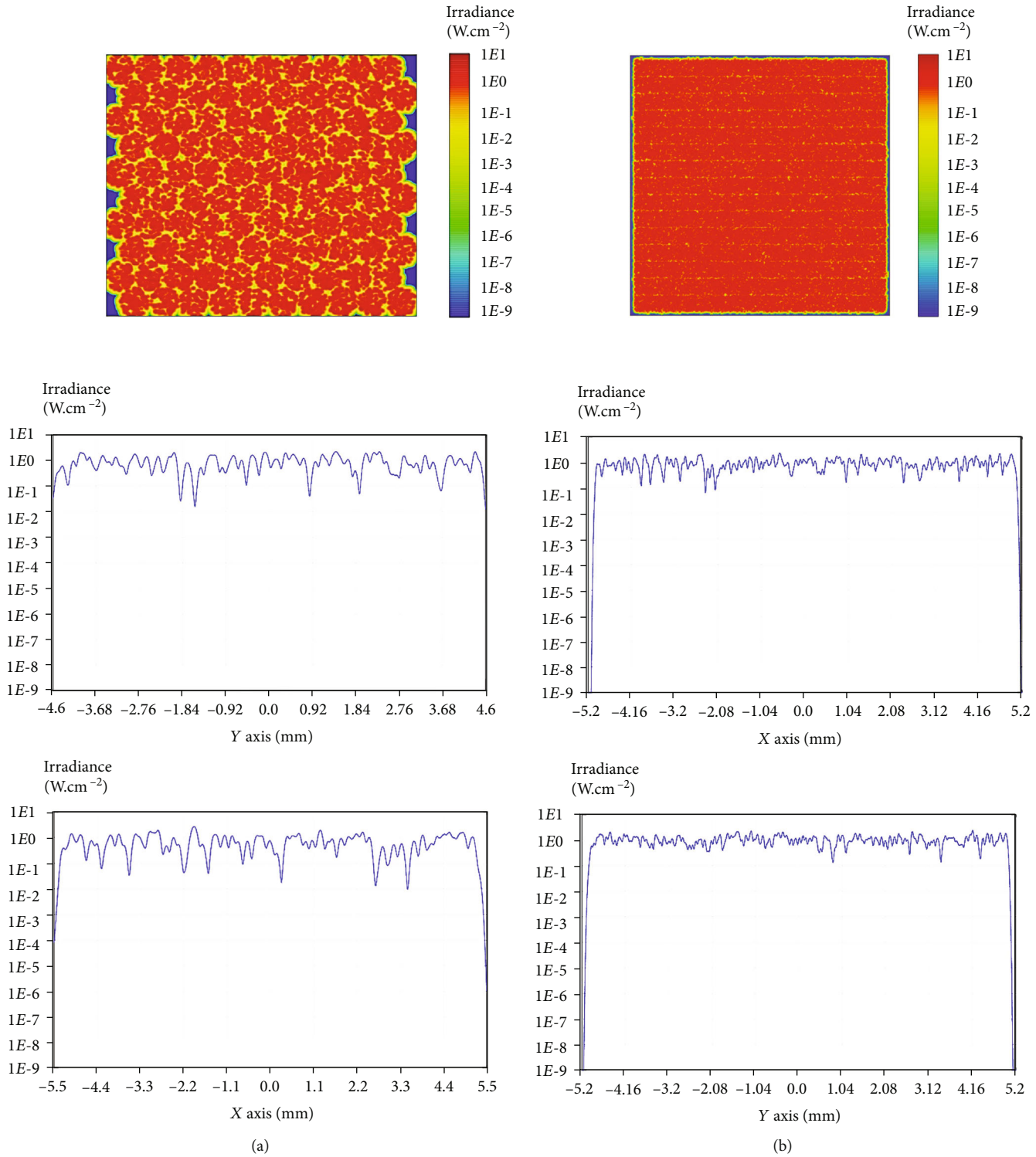

FIGURE 14: (a) Incident flux and intensity distribution in a bundle of round fibers in the X axis and Y axis and (b) in a bundle of RGOF fibers in the X axis and Y axis.

Figure 8(a) shows the source file for the spectral irradiance of the blackbody radiation at the temperature of 5780 K, and Figure 8(b) represents the direct normal irradiance of a standard solar spectrum with Air Mass 1.5 derived from standard ASTM G173-03(2012). The source file with 81 wavelengths ranging 400-1600 nm shows a close match to the direct normal irradiance of the AM 1.5 solar spectrum. The light source with a 2 mm diameter is positioned at a distance of 50 mm from the entrance aperture of the optical fiber. The light source with the wavelength range of 400 nm-1600 nm

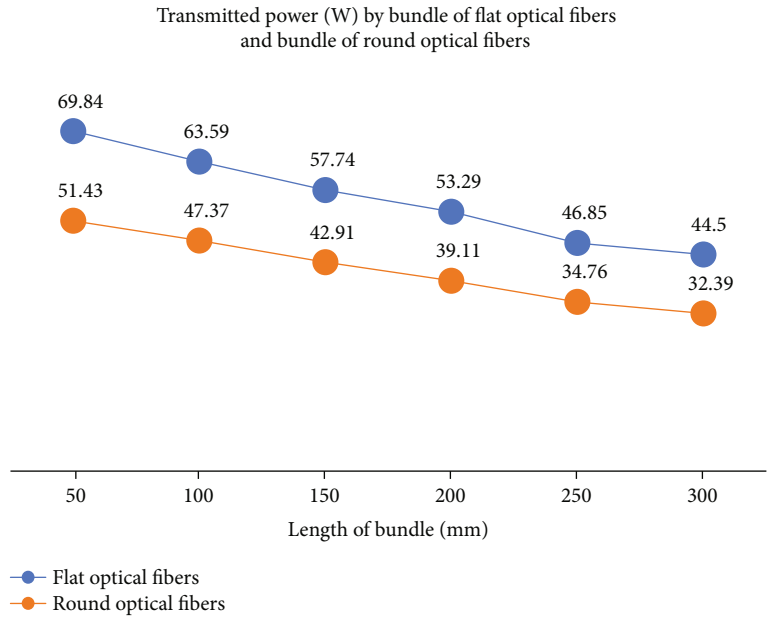

Figure 15: Comparison between power transmission by bundle of RGOF fibers and bundle of round fibers.

contains a significant part of solar spectral irradiance that is required in energy harnessing for a high concentrator photovoltaic receiver and daylighting system, where the glass optical fibers with the core material made of fused silica has a high transmission coefficient in this range.

Figure 9(a) shows the schematic diagram of the round optical fiber, and Figure 9(b) shows the schematic diagram of RGOF in the simulation. Table 1 shows the input data of the simulation for both the round optical fiber and the RGOF. The schematic diagram of simulation shows that the flat fiber does not produce skew rays. The result of the simulation shows that the leakage of the round fiber for incident angles ranging from 0° to 20° is more than that of RGOF. Figure 10 shows that the relative transmission in the round fiber is 3% less than that in RGOF for the incident angles ranging from 0° to 10°. For the incident angle between 10° and 20°, the difference of the relative transmission between the round optical fiber and the RGOF can increase up to 17% at the angle of 20°. Considering NA = 0.39 and an incident angle less than half of the acceptance angle, we conclude that the round optical fiber shows low angular loss similar to the RGOF.

To investigate the angular response and distribution of light at the endpoint of both types of fibers, Figures 11 and 12 show the simulated results at the incident angles 0°, 15°, and 25° for the round optical fiber and RGOF, respectively. The diameter of the source is 2 mm, and the maximum angle of the source with reasonable intensity and uniform output of the round optical fiber occurred at 10° which is less than half of the critical angle. Based on the results of the simulation, collimating the light before the light is transmitted via the optical fiber can increase the relative transmissions significantly for the incident angles 0° to 20°.

For the incident angles 0°-20°, the intensity of light in RGOF was higher than that in the round optical fiber. For an incident angle of 25°, the intensity of light dropped dramatically to nearly zero while the skew rays caused a maximum intensity of 4 watts per steradian in the round optical fiber. However, the amount of intensity is not considerable.

Table 2: Characteristics of a supercontinuum laser source.

Spectral coverage (nm)	500-2000
Total power (mW)	200
Total visible power (mW)	40
Polarization	Unpolarized light
Spot size (mm)	1
Output	Collimated beam

4. Investigation of the Effects of Gaps for Bundle of RGOFs and Bundle of Round Optical Fibers

In this section, we will assess the performances of the bundle of RGOFs and the bundle of round optical fibers under the same conditions. For the application of optical fibers in transmitting concentrated sunlight, the concentrator photovoltaic and daylighting (CPVD) system encounters several possible optical losses when using the bundle of optical fibers. First, the optical loss can occur during the coupling of sunlight to the aperture of the bundle of optical fibers. Second, the gap spacing between the fibers tied in a bundle can cause the energy loss when the light falls into the gaps. Third is the optical losses during the process of transmitting sunlight through optical fibers. Lastly, at the end of the fibers in a bundle, the geometrical matching between the aperture of fibers in the bundle and the dimension of the solar cell may also cause the energy loss.

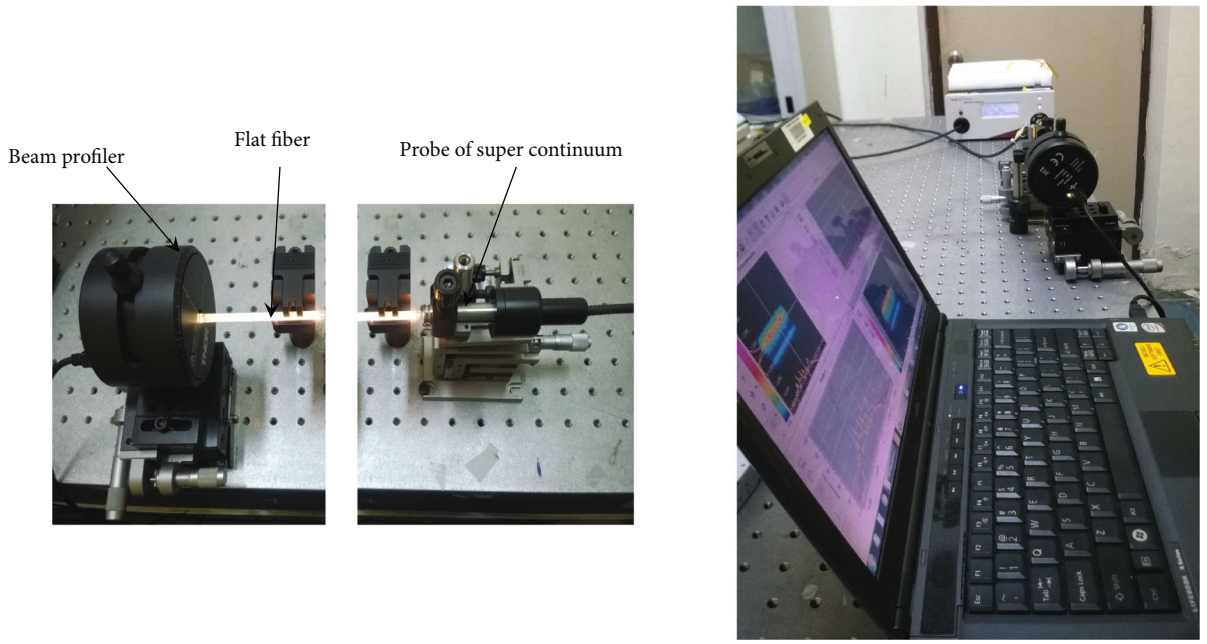

Figure 16: Setup of measuring beam profile and the photo of the cross-section of the flat fiber.

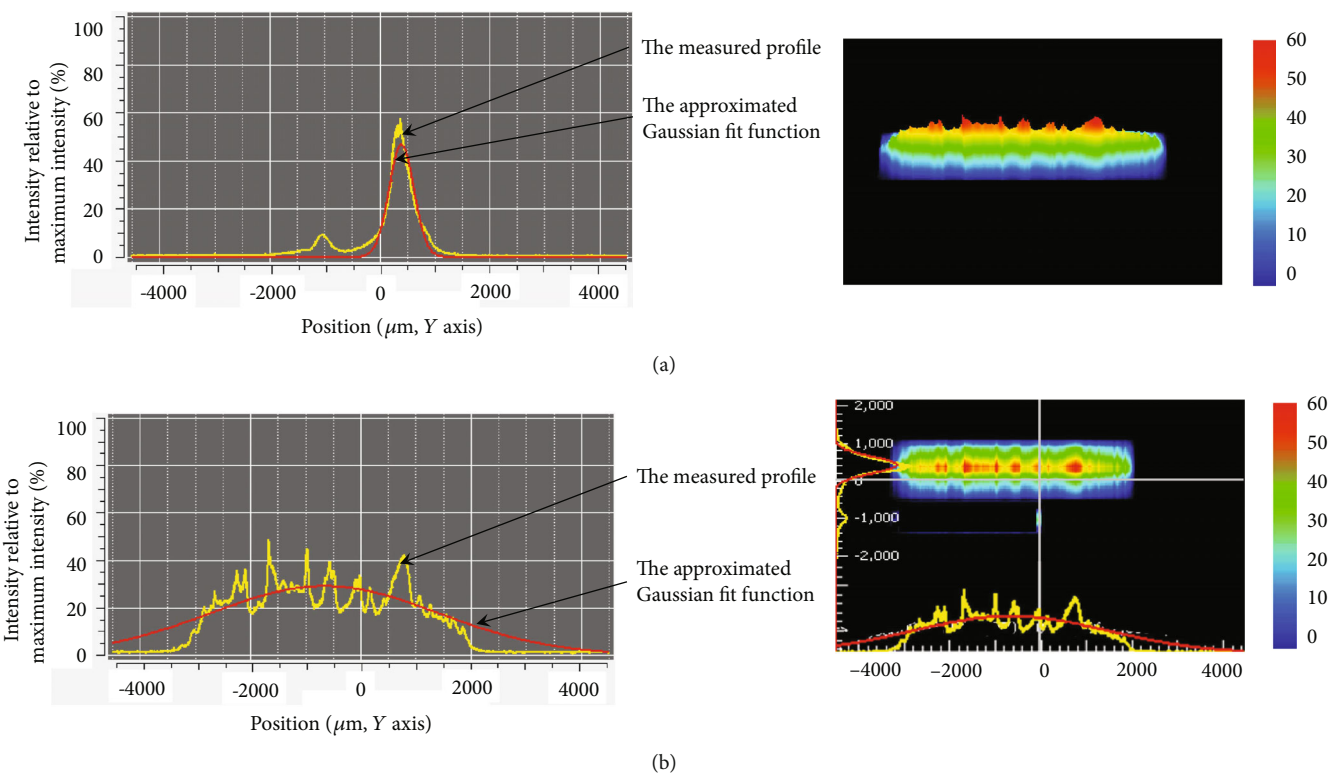

Figure 17: Profiles of the beam propagating in the flat fiber on (a) Y axis and (b) X axis.

The optical characteristics of round optical fibers and RGOFs in the bundle have been investigated using the ray-tracing method via Zemax software. To compare the performance of round and rectangular optical fibers, same core and cladding materials have been used, which are fused silica with a refractive index of 1.458464 at D-line and resin XPC-373 AP clad with a low refractive index of 1.387939 at 852nm [27]. For both cases of fibers, the propagation of light rays has been investigated at the incident angle of 0° relative to the central line of the optical fiber. A 1-watt light source based on blackbody radiation at the temperature of 5780 K (wavelengths ranging from 400 nm to 1600 nm) is applied to illuminate the bundles of optical fibers. The maximum divergence of the light source is 0.27°.

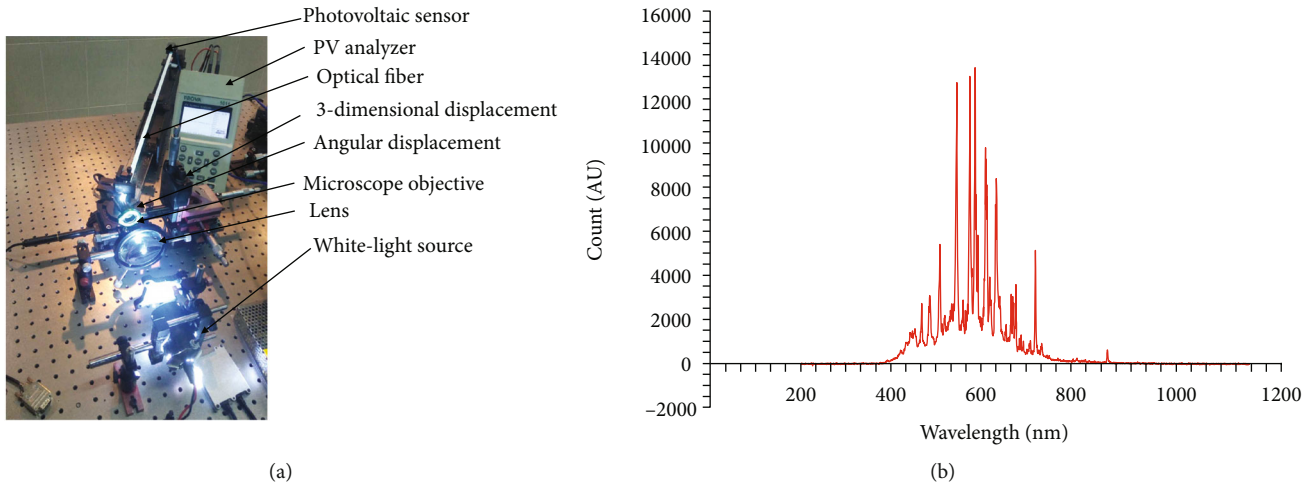

Figure 18: (a) The experiment setup of the test using a xenon lamp and (b) spectral irradiance of the xenon lamp.

Table 3: Dimensions of RGOF and round optical fiber and conditions of the test.

	RGOF	Round optical fiber
Length of optical fiber	740 mm	740 mm
Dimensions of core	Rectangle: 10 mm × 0.5 mm	Diameter: 1 mm
Diameter of focused light	1.5 mm	1.5 mm
Sensor	PV cell	PV cell
Measuring device	PV system analyzer (PROVA 1011)	PV system analyzer (PROVA 1011)
Light source	Xenon lamp H3 35 W 6000 K	Xenon lamp H3 35 W 6000 K

The active area of the photodetector is square (12 mm × 12 mm) and the thickness of the cladding is 25 μm. The area of the bundle of RGOFs was 101.6064 mm^2 while the area of the bundle of round optical fibers was 101.9172 mm^2, where the difference between the areas of both bundles is negligible, at about 0.3%. The performance including power transmission and distribution of light intensity and flux of light are evaluated in both cases. Figure 13 shows a row of fifteen units of RGOF with a cross-sectional area of 10.08 mm × 0.67 mm for each fiber to form a total cross-sectional area of 10.08 mm × 10.08 mm. The light is well mapped to the square dimension of the photodetector in both directions of X and Y. For both cases, we have applied the same testing conditions, i.e., light source, photodetector, length of fibers, material, and cross-sectional area of both-bundles. Figure 14(a) shows images of the flux on the active surface of the photodetector for both cases, and Figure 14(b) shows the intensity distribution in the X and Y directions. A comparison between the flux distributions in both cases reveals that the transmitted light rays via flat fibers are more uniform than those via round optical fibers.

Figure 15 shows the total powers for both bundles of RGOF and round optical fibers for the lengths between 50 mm and 300 mm. The result shows that the bundle of RGOF fibers transmits more power as compared to the bundle of round optical fibers because of lower optical loss at the entrance aperture of the optical fibers. The effective area of the cores in the bundle of RGOFs is 93.279 mm^2, and the effective area of the cores in the bundle of round-optical fibers is 78.539 mm^2.

5. Experimental Investigation on a Round Optical Fiber and a RGOF

With regard to the profile of the beam, relative transmission of RGOF for incident angles ranging from 0° to 25° has been investigated experimentally by using collimated white light, focused white light, and the laser beam. A supercontinuum white-light laser of NKT Photonics Company and a beam profiler by Thorlabs Company have been employed as a light source and plotter for the beam profile, respectively. Two samples of RGOF have been fabricated by using two different materials: the first sample has fused silica as the core material and the XPC 373 low refractive index polymer as the clad material; the second sample has borosilicate 3.3 as the core material and Teflon as the clad material. Table 2 lists down the characteristics of the supercontinuum laser.

Figure 16 shows the experimental setup of the beam profile measuring system, where the light source illuminates the light from one end side of the RGOF, and the beam profiler is positioned at the other end of the RGOF fiber. Figure 17(a) shows the results of the measured beam profile along the Y-axis. The intensity of light was distributed across the surface of RGOF and the maximum intensity occurred at the center of the fiber. The intensity was distributed from zero to 1000 μm along the Y-axis. The amplitude of the peak point

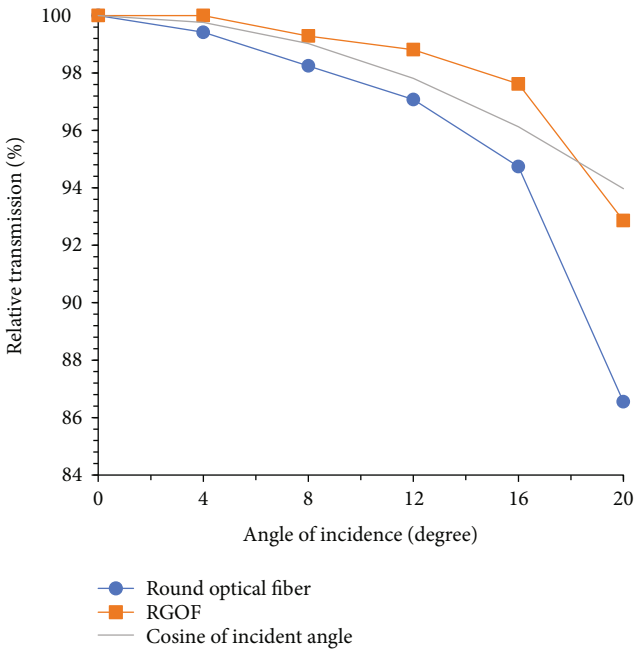

Figure 19: A comparison of relative transmission between RGOF and round optical fiber under propagation of a focused light for different incident angles.

Figure 20: Flexibility test of RGOF for bending and twisting mechanism.

was 60% of the maximum intensity set in the beam profiler. Figure 17(b) shows the measurement of the beam profiler along the X-axis.

Relative transmission of RGOF for incident angles between 0° and 20° has been measured under the propagation of a white light produced by a xenon lamp. Figure 18(a) shows the experiment setup of the test using a xenon lamp, and Figure 18(b) shows the spectral irradiance of the xenon lamp in the test that is extracted by an Ocean 2002 spectrometer. A total length of 740 mm RGOF with a cross-sectional area of 10 mm × 0.4 mm and a total length of 740 mm round optical fiber with 1 mm diameter have been fabricated for measuring the relative transmission of RGOF at different angular propagations of a focused light. Table 3 shows the conditions of the test.

Figure 19 shows that round optical fibers follow the cosine of incident light while RGOF has a higher relative transmission. The length of rectangle in RGOF is 10 mm that makes it suitable for a focused light with a diameter of less than 2 mm. The result may be used in harnessing the light around the solar cells in the receiver of a CPVD. The light at the middle of the focal plane is uniform enough for multijunction solar cells, and the light around the cells may be transmitted by bundles of RGOF.

The fabricated RGOF has just a thin layer of polymer as the clad where it has been examined with bending and twisting tests. Figure 20 shows the demonstration on the bending and twisting tests of RGOF. The fabricated fiber is bent on a cylinder with 350 mm diameter and twisted 90° along its longitude axis with a length of 2.2 m. The minimum radius of bending for the fabricated RGOF was 150 mm with a cross-sectional area of 10 mm × 0.4 mm. A lower radius may be achieved by an additional coating process.

6. Conclusion

In this study, the concept of introducing RGOF to transmit sunlight in a CPVD system is proposed and analyzed in detail. Relative transmission of RGOF for incident angles ranging from 0° to 25° has been studied via a mathematical model, numerical simulation, and experiment. The simulation result reveals that a RGOF with a cross-sectional area of 10 mm × 0.5 mm has a higher relative transmission as compared to that of a glass round optical fiber with a core diameter of 1 mm while it is exposed to the focused light with a diameter of spot size less than 2 mm. The results of experiments and simulations are limited to the collimated and focused white-light source with the spectral irradiance close to the standard solar spectrum. Moreover, the second limitation is that the relative transmission of RGOF is measured for the incident angles of light beam less than the acceptance angle of the optical fiber. A bundle of RGOFs can achieve higher efficiency in both coupling and transmitting light power as compared to a bundle of round fibers. The bundle of RGOFs has less gap spacing between fibers. The simulated result shows a good matching between of output flux distribution and the dimension of the solar cell for the case of RGOF, which is consistent with the higher coupling efficiency of RGOF. The beam profiles of both the RGOF and the round glass optical fiber under propagation of a focused light have been validated via analytical formula and numerical simulation. The profile of the output light of RGOF has

been investigated experimentally. A top-hat profile matches with the result of the propagating laser beam to the rectangular glass optical fiber. In the last section of our study, tests on the flexibility of our designed and fabricated RGOF in both bending and twisting have been carried out. In this test, RGOF can be bent with a radius of 150 mm and twisted 90° along the axis of the fiber at a fiber length of 2.2 m.

Data Availability

The data will be available upon request.

Conflicts of Interest

The authors declare that they have no conflicts of interest.

References

[1] J. Cariou, J. Dugas, and L. Martin, "Transport of solar energy with optical fibres," *Solar Energy*, vol. 29, no. 5, pp. 397–406, 1982.

[2] C. Firat and A. Beyene, "Comparison of direct and indirect PV power output using filters, lens, and fiber transport," *Energy*, vol. 41, no. 1, pp. 271–277, 2012.

[3] I. Ullah and S.-Y. Shin, "Development of optical fiber-based daylighting system with uniform illumination," *Journal of the Optical Society of Korea*, vol. 16, no. 3, pp. 247–255, 2012.

[4] C. Kandilli, K. Ulgen, and A. Hepbasli, "Exergetic assessment of transmission concentrated solar energy systems via optical fibres for building applications," *Energy and Buildings*, vol. 40, no. 8, pp. 1505–1512, 2008.

[5] A. Kribus, O. Zik, and J. Karni, "Optical fibers and solar power generation," *Solar Energy*, vol. 68, no. 5, pp. 405–416, 2000.

[6] D. Feuermann and J. M. Gordon, "Solar fiber-optic mini-dishes: a new approach to the efficient collection of sunlight," *Solar Energy*, vol. 65, no. 3, pp. 159–170, 1999.

[7] C. Sapia, "Daylighting in buildings: developments of sunlight addressing by optical fiber," *Solar Energy*, vol. 89, pp. 113–121, 2013.

[8] H. J. Han, S. B. Riffat, S. H. Lim, and S. J. Oh, "Fiber optic solar lighting: functional competitiveness and potential," *Solar Energy*, vol. 94, pp. 86–101, 2013.

[9] R. Núñez, I. Antón, and G. Sala, "Hybrid lighting-CPV, a new efficient concept mixing illumination with CPV," *Optics Express*, vol. 21, no. 4, pp. 4864–4874, 2013.

[10] D. Feuermann, J. M. Gordon, and M. Huleihil, "Solar fiber-optic mini-dish concentrators: first experimental results and field experience," *Solar Energy*, vol. 72, no. 6, pp. 459–472, 2002.

[11] B. E. Saleh and M. C. Teich, *Fundamentals of photonics*, John Wiley & Sons, 2019.

[12] A. Aslian, B. Honarvar Shakibaei Asli, C. J. Tan, F. R. M. Adikan, and A. Toloei, "Design and analysis of an optical coupler for concentrated solar light using optical fibers in residential buildings," *International Journal of Photoenergy*, vol. 2016, 11 pages, 2016.

[13] D. Feuermann, J. M. Gordon, and M. Huleihil, "Light leakage in optical fibers: experimental results, modeling and the consequences for solar concentrators," *Solar Energy*, vol. 72, no. 3, pp. 195–204, 2002.

[14] D. Kato and T. Nakamura, "Application of optical fibers to the transmission of solar radiation," *Journal of Applied Physics*, vol. 47, no. 10, pp. 4528–4531, 1976.

[15] J. M. Senior and M. Y. Jamro, *Optical fiber communications: principles and practice*, Pearson Education, 2009.

[16] C. Kandilli and K. Ulgen, "Review and modelling the systems of transmission concentrated solar energy via optical fibres," *Renewable and Sustainable Energy Reviews*, vol. 13, no. 1, pp. 67–84, 2009.

[17] J. Dugas, M. Sotom, L. Martin, and J. M. Cariou, "Accurate characterization of the transmittivity of large-diameter multimode optical fibers," *Applied Optics*, vol. 26, no. 19, pp. 4198–4208, 1987.

[18] D. Liang, Y. Nunes, L. Fraser Monteiro, M. L. F. Monteiro, and M. Collares-Pereira, "200-W solar energy delivery with optical fiber bundles," in *Proc. SPIE 3139, Nonimaging Optics: Maximum Efficiency Light Transfer IV*, San Diego, CA, United States, October 1997.

[19] K. K. Chong, T. K. Yew, C. W. Wong, M. H. Tan, W. C. Tan, and B. H. Lim, "Dense-array concentrator photovoltaic prototype using non-imaging dish concentrator and an array of cross compound parabolic concentrators," *Applied Energy*, vol. 204, pp. 898–911, 2017.

[20] H. Baig, N. Sellami, D. Chemisana, J. Rosell, and T. K. Mallick, "Performance analysis of a dielectric based 3D building integrated concentrating photovoltaic system," *Solar Energy*, vol. 103, pp. 525–540, 2014.

[21] X. Yu, Y. Su, H. Zheng, and S. Riffat, "A study on use of miniature dielectric compound parabolic concentrator (dCPC) for daylighting control application," *Building and Environment*, vol. 74, pp. 75–85, 2014.

[22] E. A. Marcatili, "Dielectric rectangular waveguide and directional coupler for integrated optics," *Bell System Technical Journal*, vol. 48, no. 7, pp. 2071–2102, 1969.

[23] V. V. Cherny, G. A. Juravlev, A. I. Kirpa, and V. R. Tjoy, "Multi-mode and single-mode optical fiber guides with rectangular core for communication systems," in *Guided wave optical systems and devices II*, International Society for Optics and Photonics, 1979.

[24] O. Blomster and M. Blomqvist, "Square formed fiber optics for high power applications," in *Proceedings of the Fourth International WLT-Conference*, Munich, Germany, 2007.

[25] K. Konishi et al., "Development of rectangular core optical fiber cable for high power laser," *SEI Technical Review*, vol. 71, pp. 109–112, 2010.

[26] S. Ambran, C. Holmes, J. C. Gates et al., "Fabrication of a multimode interference device in a low-loss flat-fiber platform using physical micromachining technique," *Journal of Lightwave Technology*, vol. 30, no. 17, pp. 2870–2875, 2012.

[27] Fospia and efiron, "Low refractive index XPC-series," 2019, https://www.fospia.com/xpc-series.